

# High Molecular Orientation in Mono- and Trilayer Polydiacetylene Films Imaged by Atomic Force Microscopy

Darryl Y. Sasaki,<sup>1</sup> Robert W. Carpick,<sup>2</sup> and Alan R. Burns

*Biomolecular Materials and Interface Science Department, Sandia National Laboratories, Albuquerque, New Mexico 87185-1413*

Received December 22, 1999; accepted June 12, 2000

**Atomically flat monolayer and trilayer films of polydiacetylenes have been prepared on mica and silicon using a horizontal deposition technique from a pure water subphase. Langmuir films of 10,12-pentacosadiynoic acid (I) and *N*-(2-ethanol)-10,12-pentacosadiynamide (II) were compressed to 20 mN/m and subsequently polymerized by UV irradiation at the air–water interface. Blue and red forms of the films were prepared by varying exposure times and incident power. Polymerization to the blue-phase films produced slight contractions of 2 and 5% for the films of II and I, respectively. Longer UV exposures yielded red-phase films with dramatic film contraction of 15 and 32% for II and I, respectively. The horizontal deposition technique provided transfer ratios of unity with minimal film stress or structure modification. Atomic force microscopy images revealed nearly complete coverage of the substrate with atomically flat films. Crystalline domains of up to 100 micrometers of highly oriented polydiacetylene molecules were observed. The results reported herein provide insight into the roles of molecular packing and chain orientations in converting the monomeric film to the polymerized blue and red phases.** © 2000 Academic Press

**Key Words:** polydiacetylene; Langmuir films; AFM; horizontal deposition; molecular orientation.

## INTRODUCTION

Polymerization of oriented mono- and multilayer structures containing diacetylene functionality has produced an assortment of colored, robust, highly oriented, and environmentally responsive films (1). These two-dimensional polydiacetylene films, where the conjugation runs parallel to the film surface, have been prepared as Langmuir monolayers (2), Langmuir–Blodgett (LB) multilayer films (3), bilayer systems (4), and self-assembled monolayers (SAM) (5). Numerous applications for these films have been explored, including biomimetic surfaces for protein studies (6), biosensors (7), NLO materials (8), and biomineralization templates (9).

These materials exhibit high structural order in the many different forms yielding colored films that range from blue to

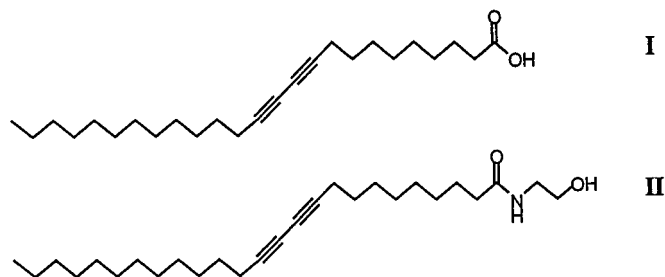
red. The color of each material results from the conformation of the conjugated backbone. The conformation is in turn affected by the orientation and packing of the hydrocarbon side chains pendant to the backbone that can either alter the length or change the mode of  $\pi$  conjugation (10). A variety of analytical techniques, such as electron diffraction (11), Fourier transform infrared spectroscopy (12), resonance Raman (13), and fluorescence polarization (14), have been employed to identify the molecular orientation of the side chains and backbones.

Recently, atomic force microscopy (AFM) has been used to image polydiacetylene films at the nanometer scale to evaluate film structure based on topography (15), friction anisotropy (16), and surface features (12, 17, 18). Although the technique is quite powerful, the images reveal a wide range in film quality. Previous work involving LB films of polydiacetylenes required the use of metal ion salts (e.g., CdCl<sub>2</sub>, CaCl<sub>2</sub>) to stabilize the carboxylic acid headgroups for deposition of the monolayer (3, 18, 19). The use of metal ion salts, however, can complicate the structures by either altering molecular orientation through metal ion chelation (14, 20) or by depositing salt crystals in or on the LB film.

In this paper, we will describe the formation of mono- and trilayer films of polydiacetylenes polymerized at the air–water interface on a pure water subphase. The colored films were subsequently transferred onto mica, silicon, or glass substrates using a horizontal deposition technique to capture innate features in the polymerized films. For the carboxylic acid functionalized amphiphile, 10,12-pentacosadiynoic acid (**I**), a stable trilayer structure was prepared on the pure water subphase through overcompression of the monolayer. Stable monolayers of **I** could not be obtained in the absence of metal ion salts. Stable polydiacetylene monolayers could, however, be prepared in the absence of salts using an ethanolamido functionalized analog of **I**, *N*-(2-ethanol)-10,12-pentacosadiynamide (**II**) (Scheme 1). The amide functionality adds stability to the monolayer through lateral intermolecular hydrogen-bonded networks at the headgroup position. The deposited films were subsequently characterized with AFM and fluorescence microscopy to reveal highly oriented crystalline-like domains that extend for tens to hundreds of micrometers for both monolayer and trilayer films. Film shrinkage and changes in film height upon UV-induced polymerization indicated a reorganization of the alkyl side chains as the film transitions from the blue to red phase.

<sup>1</sup> To whom correspondence should be addressed. Fax: (505) 844-5470. E-mail: [dysasak@sandia.gov](mailto:dysasak@sandia.gov).

<sup>2</sup> Present address: Department of Engineering Physics, University of Wisconsin–Madison, 1500 Engineering Drive, Madison, WI 53706.



SCHEME 1

## MATERIALS AND METHODS

All solvents for purification and synthesis were of reagent grade (Fisher) and used as received. Solvents for monolayer spreading were of spectroscopic grade. The monolayer subphase was pure water (resistivity  $\geq 18 \text{ M}\Omega\text{-cm}$ ) filtered through a Barnstead Nanopure system (Dubuque, IA). NMR analyses were performed on a Bruker AMX 400 (Fremont, CA). Infrared absorption spectra were taken on a Perkin–Elmer 1750 FTIR spectrometer (Norwalk, CT). UV–vis spectral data were collected on a Perkin–Elmer Lambda 19 spectrophotometer. Elemental analyses were performed by Desert Analytics (Tucson, AZ).

10,12-Pentacosadiynoic acid (**I**) was obtained from Farchan/GFS Chemicals (Powell, OH) as a bluish powder. The powder was taken up in a small amount of ethyl acetate and passed through a silica gel column with 25% ethyl acetate/hexanes ( $R_f = 0.23$ ). The appropriate fractions were collected and evaporated to dryness below room temperature to minimize polymerization of the diacetylene monomer. A white powder was isolated and stored at  $-20^\circ\text{C}$ , protected from light.

To prepare *N*-(2-ethanol)-10,12-pentacosadiynamide (**II**), oxalyl chloride (0.64 mL, 0.93 g, 7.3 mmol) was added dropwise to a solution of **I** (2.50 g, 6.67 mmol) in  $\text{CH}_2\text{Cl}_2$  (50 mL). The initial gas evolution subsided after 1 h of stirring, and then a drop of DMF was added to complete the reaction. Following another hour of stirring, the solution was evaporated to dryness and the residuals dissolved in a mixture of THF (40 mL) and ethanolamine (1.61 mL, 1.63 g, 26.7 mmol). After stirring overnight, ethyl acetate (60 mL) and  $\text{H}_2\text{O}$  (60 mL) were added to the reaction mixture, the mixture was shaken, the layers were separated, and the aqueous layer was extracted with fresh ethyl acetate ( $2 \times 60 \text{ mL}$ ). The organics were combined and washed with  $\text{H}_2\text{O}$  (60 mL), followed by aqueous saturated  $\text{NaHCO}_3$  (60 mL) and then brine (60 mL). The organic layer was isolated and further dried over anhydrous  $\text{MgSO}_4$ , filtered, and then concentrated *in vacuo*. The residuals were flash column chromatographed on silica gel (ethyl acetate,  $R_f = 0.18$ ). **II** was isolated as a white powder. Over time the compound developed a slight blue tinge even in storage at  $-20^\circ\text{C}$ , protected from light. All spectral and elemental analysis data were identical with those reported in the literature (21).

All  $\pi$ -*A* isotherms and Langmuir film preparations were performed on a Nima 2011 circular Langmuir trough (Coventry, England). The trough was situated on a vibration isolation table inside a class 100 clean room. The pure water subphase was kept at a temperature of  $15 \pm 0.2^\circ\text{C}$ . Diacetylene monomers were spread on the water surface in a 50% chloroform/benzene solution. While solutions of **I** were completely homogeneous, solutions of **II** needed to be passed through a  $0.2\text{-}\mu\text{m}$  filter to remove small traces of red polymer and then diluted to volume. All films were incubated for 10–15 min at zero pressure prior to compression. The compression rate for the  $\pi$ -*A* isotherms and for LB preparation was  $100 \text{ cm}^2/\text{min}$  ( $4 \text{ \AA}^2/\text{molecule} \cdot \text{min}$ ).

For UV polymerization at the air–water interface, the Langmuir films were compressed to a surface pressure of  $20 \text{ mN/m}$  and equilibrated at that pressure for 20–30 min. Within the first 5–10 min the films stabilized to a constant molecular area. UV irradiation of the compressed films was performed with two Oriel pen lamps laterally spaced 8 cm apart. Their combined incident power output directly below the center of the lamps at various distances are shown in Table 1. The lamps were set to particular heights above the air–water interface and the films irradiated for fixed time periods (Table 1) to yield blue- or red-phase films. After the lamps were turned off, the films sat undisturbed for a few minutes, and then the water was slowly drained off by aspiration. The monolayers were laid down on mica (freshly cleaved), silicon (piranha cleaned), or glass substrates (piranha cleaned) that had been submerged horizontally in the aqueous subphase prior to monolayer spreading. After the monolayer was securely deposited on the substrate, the substrate was removed by forceps and allowed to dry in the clean room.

A Nanoscope IIIA AFM (Digital Instruments, Santa Barbara, CA) operating in contact mode was used to obtain topographic images. Measurements with the AFM were acquired under laboratory ambient conditions. The scan rate was 3 Hz (=lines/s) unless otherwise noted. Silicon nitride cantilevers (Digital Instruments) with a nominal normal force constant of  $0.06 \text{ N/m}$  were used for all measurements.

Microscopic (far-field) sample fluorescence of red-phase films was recorded using a Leitz optical fluorescence microscope equipped with dichroic beam filters and polarized white light from a xenon lamp. The sample was illuminated with 520–550 nm light, and emission wavelengths greater than 590 nm were passed to a CCD camera, which captured the field of view for the images.

## RESULTS AND DISCUSSION

Amphiphiles of **I** and **II** on pure water produced the pressure–area ( $\pi$ -*A*) isotherms shown in Fig. 1. Both films gave nearly identical take-off areas from zero pressure of  $25 \text{ \AA}^2/\text{molecule}$ , corresponding to the molecular cross section of the hydrocarbon–diacetylene structure. The film of **I** collapses at low pressure ( $\sim 12 \text{ mN/m}$ ), but upon overcompression reaches a stable solid phase showing a limiting molecular area of

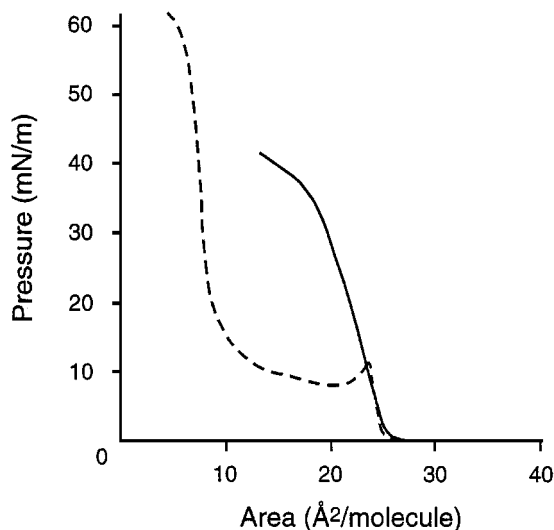


**FIG. 1.** Pressure–area ( $\pi$ – $A$ ) isotherms of **I** (---) and **II** (—) diacetylene compounds on a pure water subphase at 15°C.

$\sim 8 \text{ \AA}^2/\text{molecule}$ . This overcompressed state corresponds to a stable trilayer structure (20). The film of **II** was stable as the monolayer with a collapse pressure of ca. 35 mN/m and an extrapolated molecular area at zero pressure of  $25 \text{ \AA}^2/\text{molecule}$ .

Both diacetylene films were polymerized at the air–water interface and deposited onto solid substrates using the horizontal deposition method described below. Films equilibrated at 20 mN/m were polymerized to the blue phase by exposure to incidence powers of  $40 \mu\text{W}/\text{cm}^2$  for **I** and  $23 \mu\text{W}/\text{cm}^2$  for **II** over a period of 30 s (Table 1). Red-phase films were produced by exposing the trilayer of **I** to  $500 \mu\text{W}/\text{cm}^2$  and the monolayer of **II** to  $40 \mu\text{W}/\text{cm}^2$  for 5 min.

Upon UV exposure, the diacetylene films not only changed color but also shrank with increasing exposure times (Table 1). Both films of **I** and **II** contracted slightly in area by 5 and 2%, respectively, upon conversion to the blue-phase. Conversion to the red-phase, on the other hand, dramatically contracted the films by 32% for **I** and 15% for **II**. The contraction observed for **II** is consistent with that observed for similar diacetylene

**TABLE 1**  
**UV Polymerization of Diacetylene Films at the Air–Water Interface<sup>a</sup>**

Amphiphile	Exposure time	Lamp height (cm)	Incident power <sup>b</sup> ( $\mu\text{W}/\text{cm}^2$ )	Film color	% Area contraction
<b>I</b>	30 s	10	40	Blue	5
<b>I</b>	5 min	6	500	Red	32
<b>II</b>	30 s	15	23	Blue	2
<b>II</b>	5 min	10	40	Red	15

<sup>a</sup> At 20 mN/m surface pressure on a pure water subphase maintained at 15°C.

<sup>b</sup> Determined using Model 365 exposure analyzer (Optical Associates Inc.), with a maximum absorption at 260 nm.

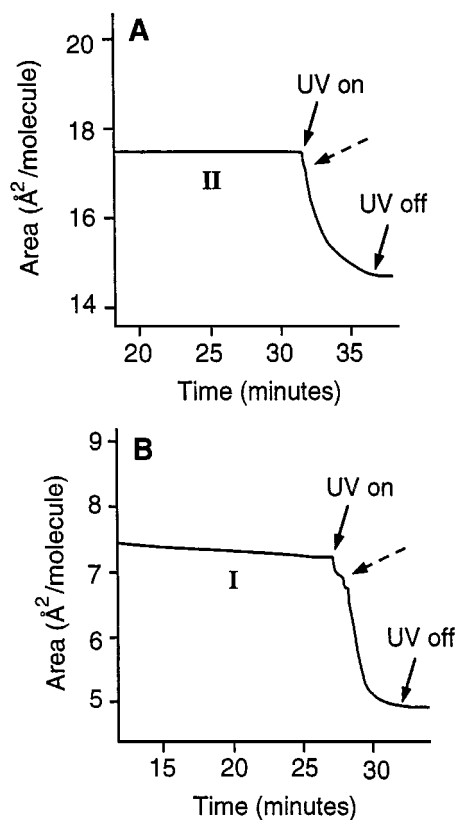


**FIG. 2.** Plots of molecular area vs time of **II** (A) and **I** (B) films maintained at a surface pressure of 20 mN/m on a pure water subphase at 15°C, prior to and during a 5-min UV irradiation exposure. Dotted arrows indicate the point at which pseudostable blue-phase structures exist. The time axis shown is a portion of the total curve that begins from the film compression followed by pressure equilibration and finally UV exposure.

monolayers in the literature (3, 14, 20). However, the behavior of the **I** trilayer is unique. Figures 2A and 2B shows the area vs time plots for mono- and trilayer films of **II** and **I**, respectively, prior to and during a 5 min UV exposure. Both films reach stable structures at a constant surface pressure of 20 mN/m prior to UV irradiation. Immediately following the onset of UV irradiation, the films began to contract. Interestingly, in the first 30 s of UV irradiation both films reach a metastable blue-phase structure, where the molecular area shows signs of leveling off (dotted arrows in Figs. 2A and 2B). With further exposure the films then continue to contract as they progressively convert to the red form. Within the first 3 min of exposure more than 90% of the total contraction has occurred. After 4 min, the films have reached stable structures. All polymerizations were conducted in clean-room air and no expansion of the monolayer was observed at any time before, during, or after UV exposure (20).

The polymerized films were then transferred onto solid substrates for further characterization. Initially, we attempted to deposit the films using a vertical dipping LB deposition technique. However, the very rigid nature of the films, especially in the blue phase, prevented any reasonable film transfer. Typically,

for the blue films of both **I** and **II**, only a few small ( $<1\text{ cm}^2$ ) film fragments would break off and transfer onto the substrate ( $4 \times 2.5\text{ cm}$ ). Because of the crystalline-like structure of the blue films, the total area would remain constant at a pressure of  $20\text{ mN/m}$ , but a visible hole in the film would persist where the transfer took place. Unlike the homogeneously continuous and stiff blue-phase films, the red-phase films had visible cracks throughout. This allowed the film to compress with vertical deposition so that film transfer was significantly improved. However, even in this case the transfer was less than 70% and the film exhibited oriented features induced from the transfer process.

To capture the innate features of the polymerized films on the pure water subphase, as well as achieving high transfer ratios, a horizontal deposition method was employed. Substrates were situated on a support at a depth of  $1\text{--}2\text{ mm}$  below the air–water interface and oriented plane-parallel to the surface. Following UV exposure, the film was transferred onto the solid substrate by lowering the water level by aspiration. Once the film draped over the substrate, excess film was removed from the outside edges of the substrate using the aspirator. The substrate was removed and the trapped water between the film and substrate was allowed to evaporate in clean-room air. Visual inspection indicated no macroscopic changes in the transferred blue- and red-phase films relative to their appearance on the air–water interface.

UV–vis spectra of the polydiacetylene films were typical of blue- and red-phase forms. Figure 3 displays the absorption spectra of poly(**I**) trilayer films after  $30\text{ s}$  at  $40\text{ }\mu\text{W/cm}^2$  (blue-phase) and one after a  $5\text{-min}$  exposure at  $500\text{ }\mu\text{W/cm}^2$  (red-phase). Poly(**II**) monolayer films gave nearly identical spectra although with about 70% less intensity, as would be expected for a sample one-third the thickness of the poly(**I**) trilayer.

AFM images of the blue- and red-phase forms of poly(**I**) and poly(**II**) on mica are shown in Fig. 4. The coverage for all

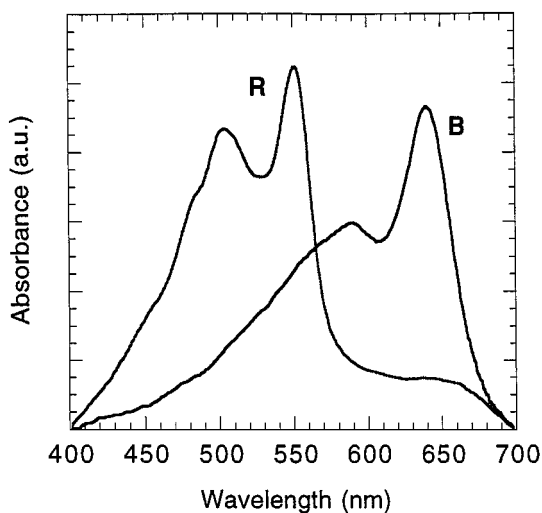


**FIG. 3.** UV–vis absorption spectra of blue-phase (B) and red-phase (R) poly(**I**) trilayer films deposited on glass substrates.

films was nearly uniform for the entire mica substrate. The topographic images in Fig. 4 are of areas with cracks or defects in the film to allow for some contrast. Over 95% of the transferred film was flat to within  $2\text{--}3\text{ \AA}$  with up to  $100\text{-}\mu\text{m}$  crystalline-like domains observed. Films produced on silicon substrates with both native and thermally grown oxide possessed the same quality.

The choice of a pure water subphase was a result of our initial attempts to prepare mono- and multilayer films using metal ion salts of **I**.  $\text{CdCl}_2$  and  $\text{CaCl}_2$  salts, at concentrations from  $1\text{ }\mu\text{M}$  to  $3\text{ mM}$ , were used in the subphase to prepare stable monolayers of **I**. Following both vertical and horizontal deposition, AFM images revealed micrometer-scale salt crystals dispersed throughout the samples. An example of such an image is shown in Fig. 5. It was clear that such contaminated films would not be amenable to any molecular level studies, not only because of the surface roughness produced by the crystallites, but also from their effects on the chromatic molecular actuation of the film (15).

The  $50\text{-}\mu\text{m}$  images of the films formed on pure water subphase show overall polydiacetylene morphology and film structure (Fig. 4). For the blue-phase film of **I**, square edges and straight-line cracks were observed giving the film a crystalline-like morphology (Fig. 4A). In the red-phase films of **I** (Fig. 4B), straight-line cracks were also observed, but not always with square edges. Some curved cracks were also present. The increased number of cracks compared with the blue-phase films was coincident with the film contraction that was observed on the trough.

Polarized fluorescence microscopy of the red films has shown that the polydiacetylene backbones in a single domain are highly oriented (15). By setting the analyzing polarizers at  $90^\circ$  to the backbone direction the emission of a given trilayer domain could be extinguished by a factor of at least 100. This confirms that the conjugated backbones within each domain are highly ordered and that there is structural registry between the three layers of the red phase of **I**. Thus, the crystallinity of the domains exists not only parallel to the substrate, but normal to it as well. Similarly, high polarization contrast was also observed for fluorescence from the red-phase film of **II**, indicating that the backbones are also highly oriented in the monolayer. AFM imaging also confirms the presence of straight-line cracks in films of **II** (Figs. 4C and 4D), although far fewer cracks are observed than with films of **I**. These results indicate a high degree of crystalline ordering in all films.

AFM imaging could also resolve structural differences between the blue- and red-phase films of both **I** and **II**. Distinct height differences (relative to bare substrate) between the blue- and red-phase trilayer stacks of poly(**I**) were measured at  $7.4 \pm 0.8$  and  $9.0 \pm 0.9\text{ nm}$ , respectively. Similarly, the blue- and red-phase poly(**II**) monolayer films exhibited proportional height differences of  $2.7 \pm 0.3$  and  $3.1 \pm 0.3\text{ nm}$ , respectively.

Figure 6 shows higher resolution views of the blue-phase films for **I** and **II** revealing the molecular orientation and highly regular structures within the materials. We have previously determined that the striated patterns observed in Fig. 6 run

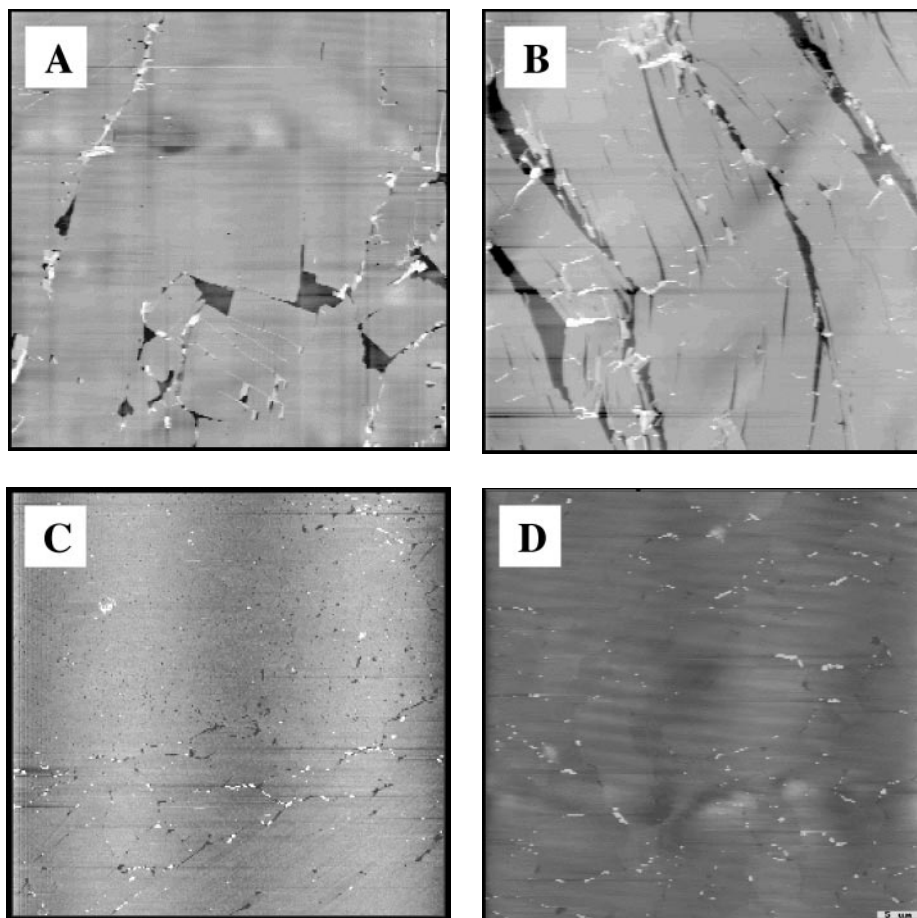


**FIG. 4.** 50- $\mu\text{m}$  topographic AFM images of poly(I) in the blue phase (A) and red phase (B) and poly(II) in the blue phase (C) and red phase (D) on mica.

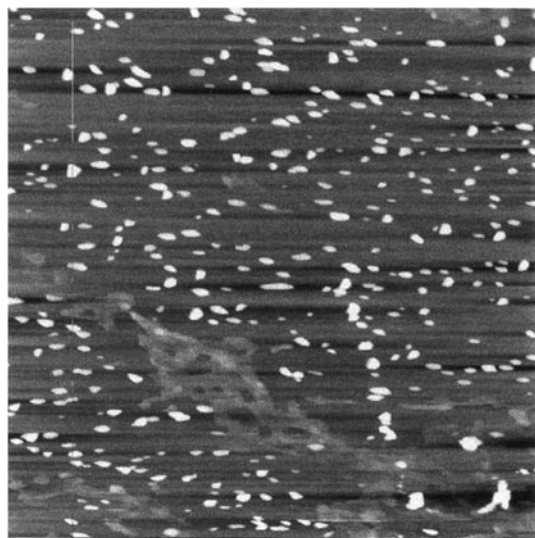


**FIG. 5.** 50- $\mu\text{m}$  topographic AFM image of horizontally deposited poly(I) monolayer from an aqueous 1 mM  $\text{CdCl}_2$  subphase on mica. Numerous micron scale crystallites (white dots) cover the surface.

parallel to the polydiacetylene backbone (15, 16). Each defined line feature was 10–20 nm wide, indicating that a set of 20–40 polymers created a single feature. The height contrast was  $\sim 0.2$  nm. The origin of these features is not fully understood. It is possible that they arise from slightly different packing densities of groups of neighboring backbones. In any event, this topographic contrast clearly reveals the highly oriented nature of the backbones within each domain. In addition, we have obtained preliminary AFM images revealing molecular lattice resolution, similar to more detailed results of Lio *et al.* (12). With such highly oriented films, nanometer-scale structures can be readily and reproducibly imaged. The high quality of these films has allowed us to observe dramatic properties such as nanometer scale conversion from blue to red by mechanical stress (15) and strong friction anisotropy (16).

These results provide insight into the possible molecular orientation of diacetylene films as they convert from monomeric to blue- and red-phase polymer structures. The headgroup interactions and alkyldiyne chain stacking should dominate the film structure of the monomeric diacetylene Langmuir films. The ability of the amide headgroup of **II** to form intermolecular hydrogen-bonded structures (Fig. 7), similar to  $\beta$ -sheets in

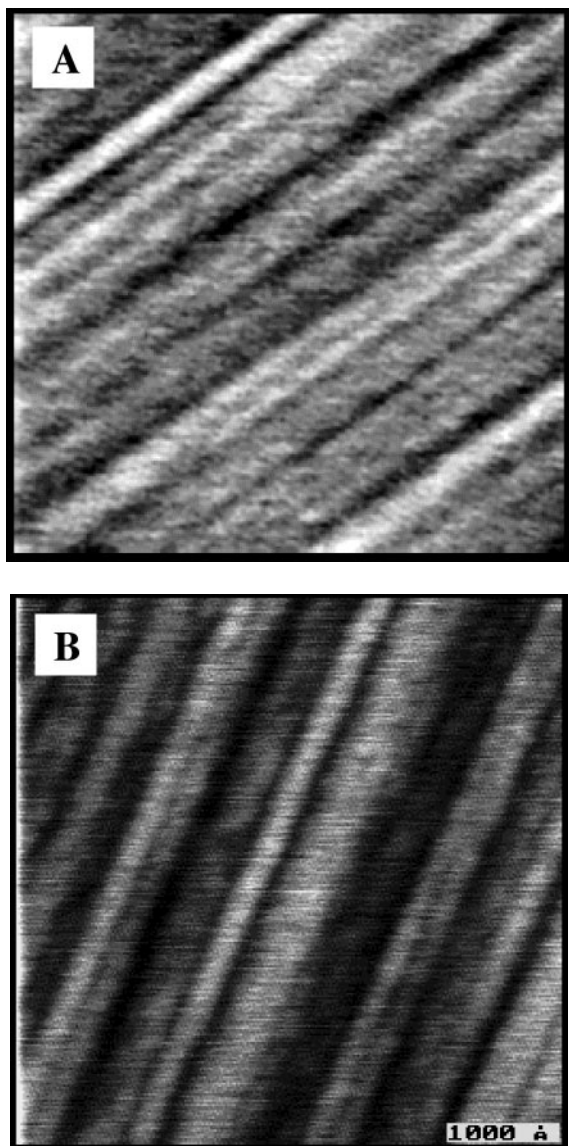


**FIG. 6.** High-resolution 1- $\mu\text{m}$ -scale topographic AFM image of blue-phase poly(I) (A) and poly(II) (B) showing highly oriented film structure (on mica). The height contrast of the striations is 0.2 nm.

proteins, may explain the stability of this monolayer film on pure water. **I** films on a pure water subphase, on the other hand, are unstable as monolayers but stack favorably into trilayer structures. Carboxylic acid dimer formation may aid in stabilizing the structure (Fig. 7). Indeed, stable bilayer islands are commonly observed on top of the **I** trilayer.

The high registry of the diacetylene packing permits rapid topochemical polymerization of the diyne monomers to the ene-yne conjugation upon UV illumination, resulting in the blue-phase polydiacetylene. Little change in the amphiphile packing, and thus little reorientation of the alkyl side chains occurs, as evidenced by the minimal contraction of the film (Table 1). However, the hybridization change from  $sp$  to  $sp^2$  for the terminal alkyne carbons creates a stress on the polymer as a result of the

$180^\circ$  to  $120^\circ$  bond angle conversion (see Fig. 7) (22). At low polymer conversion the conformational stress may be alleviated through the flexibility of neighboring monomeric or low molecular weight polydiacetylene chains. However, as the degree of polymerization of the polydiacetylene increases with UV illumination, the overall molecular stress in the film continues to increase. At some high degree of polymerization the film's original structure breaks down as the alkyl chains of the blue-phase

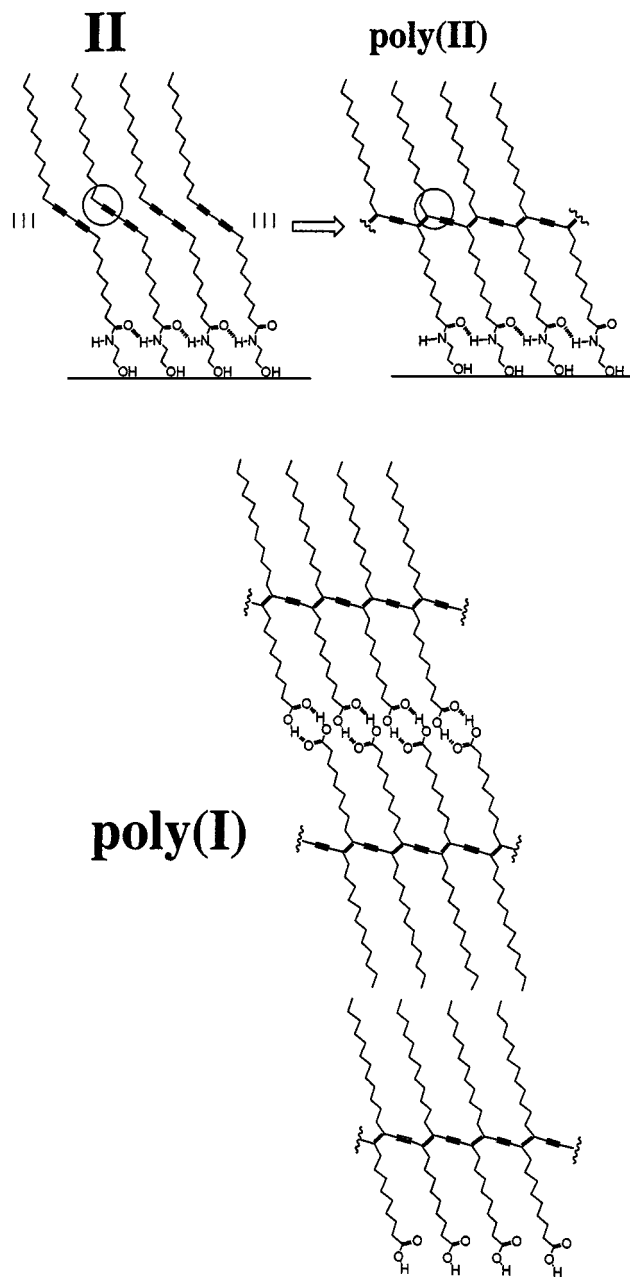


**FIG. 7.** Schematic of molecular orientation of **II** and its subsequent conversion to poly(**II**) upon UV irradiation (above). A hybridization change going from the diyne to ene-yne arrangement is circled to show the  $180^\circ$  to  $120^\circ$  bond angle conversion. A hydrogen-bonded network at the headgroup position is also drawn for the film of **II**. Below is a illustration of poly(**I**) in its trilayer form.

polymer reorganize to accommodate the bond angle conversion, yielding a closer packing (film contraction) and reorientation (vertical height enhancement) of the alkyl chains. This reorganization, although thermodynamically more stable, produces a loss of  $\pi$  conjugation and results in the red form of the polydiacetylene (13, 19, 23). We are currently investigating the alkyl side chain reorientation by coupling molecular modeling with experimental studies to further understand the color transitions and modes of actuation of these films.

### CONCLUSION

Highly oriented, crystalline-like polydiacetylene mono- and trilayer films of **II** and **I**, respectively, have been prepared in both blue and red forms using a horizontal deposition technique from a pure water subphase. Due to the stiffness of the polymerized films, orientation of the substrate, and mild conditions of the deposition, we believe the features in the film to be identical to those formed on the air–water interface. AFM imaging showed nanometer-scale striations in the films that extended throughout crystalline-like domains that reached 100- $\mu\text{m}$ . Through the observed contractions in the films on the air–water interface upon conversion from monomeric to blue phase and then to red-phase polydiacetylene, and AFM height measurements of those films, it appears that significant and spontaneous reorganization of the films occurs during UV illumination involving reorientation of alkyl chains. These molecularly flat films have allowed us to investigate chromatic transitions of polydiacetylene at the nanometer level.

### ACKNOWLEDGMENTS

We thank Dr. Mary Crawford for the power measurement readings of the UV pen lamps, and Dr. Seema Singh for the AFM image of Fig. 5. R.W.C. acknowledges the support of the Natural Sciences and Engineering Research Council of Canada. Sandia is a multiprogram laboratory operated by Sandia

Corporation, a Lockheed Martin Company, for the United States Department of Energy under Contract DE-AC04-94AL85000.

### REFERENCES

1. Bloor, D., and Chance, R. R., "Polydiacetylenes," Nijhoff, Boston, 1985.
2. Wilson, T. E., and Bednarski, M. D., *Langmuir* **8**, 2361 (1992).
3. Kuriyama, K., Kikuchi, H., and Kajiyama, T., *Langmuir* **12**, 6468 (1996).
4. Charych, D. H., Nagy, J. O., Spevak, W., and Bednarski, M. D., *Science* **261**, 585 (1993).
5. Kim, T., Chan, K. C., and Crooks, R. M., *J. Am. Chem. Soc.* **119**, 189 (1997).
6. Bader, H., van Wagenen, R., Andrade, J. D., and Ringsdorf, H., *J. Colloid Interface Sci.* **101**, 246 (1984).
7. Charych, D., and Nagy, J. O., *Chem.-Tech.* **26**, 24 (1996).
8. Sarkar, A., Okada, S., Nakanishi, H., and Matsuda, H., *Macromolecules* **31**, 9174 (1998).
9. Litvin, A. L., Samuelson, L. A., Charych, D. H., Spevak, W., and Kaplan, D. L., *J. Phys. Chem.* **99**, 12065 (1995).
10. Rughooputh, S. D. D. V., Bloor, D., Phillips, D., Jankowiak, R., Schütz, L., and Bässler, H., *Chem. Phys.* **125**, 355 (1988).
11. Day, D., and Lando, J. B., *Macromolecules* **13**, 1483 (1980).
12. Lio, A., Reichert, A., Ahn, D. J., Nagy, J. O., Salmeron, M., and Charych, D. H., *Langmuir* **13**, 6524 (1997).
13. Saito, A., Urai, Y., and Itoh, K., *Langmuir* **12**, 3938 (1996).
14. Miyano, K., and Mori, A., *Thin Solid Films* **168**, 141 (1989).
15. Carpick, R. W., Sasaki, D. Y., and Burns, A. R., *Langmuir* **16**, 1270 (2000).
16. Carpick, R. W., Sasaki, D. Y., and Burns, A. R., *Tribology Lett.*, in press.
17. Marti, O., Ribi, H. O., Drake, B., Albrecht, T. R., Quate, C. F., and Hansma, P. K., *Science* **239**, 50 (1988).
18. Sheth, S. R., and Leckband, D. E., *Langmuir* **13**, 5652 (1997).
19. Collins, M., *J. Poly. Sci. B Polym. Phys.* **26**, 367 (1988).
20. Day, D., and Ringsdorf, H., *J. Polym. Sci. Polym. Lett.* **16**, 205 (1977).
21. Wilson, T. E., Spevak, W., Charych, D. H., and Bednarski, M. D., *Langmuir* **10**, 1512 (1994).
22. Menzel, H., Mowery, M. D., Cai, M., and Evans, C. E., *J. Phys. Chem. B* **102**, 9550 (1998).
23. Tomioka, Y., Tanaka, N., and Imazeki, S., *J. Chem. Phys.* **91**, 5694 (1989).